An OFDM Sensing Algorithm in Full-Duplex Systems with Self-Interference and Carrier Frequency Offset

Qingqing Cheng, Zhenguo Shi, Diep N. Nguyen, Eryk Dutkiewicz
School of Electrical and Data Engineering, University of Technology Sydney, Sydney, Australia
{Qingqing.Cheng, Zhenguo.Shi}@student.uts.edu.au, {Diep.Nguyen, Eryk.Dutkiewicz}@uts.edu.au

***Abstract*—Full duplex (FD) wireless technology, which enables simultaneous transmission and reception on the same frequency, has shown its great potential for doubling the spectral efficiency as well as spectrum sensing while transmitting in cognitive radio networks (CRNs). However, the self-interference (SI) suppression, the underlying technique of FD, is often imperfect, resulting in non-negligible residual SI that severely affects the test statistics of sensing methods. The residual SI thereby significantly deteriorates the spectrum sensing accuracy. In this work, we aim to address this issue by proposing a novel sensing approach in FD systems leveraging the Pilot-Tone (PT) structure of Orthogonal Frequency Division Modulation (OFDM) signals. In comparison with the conventional sensing methods in FD systems, the developed sensing approach holds the advantage in the robustness not only to residual SI but also the carrier frequency offset (CFO). Besides, the proposed sensing method is able to accomplish sensing tasks in low SNR conditions with much lower computational complexity. Numerical simulations results demonstrate that the probability of detection of our proposed approach can be improved up to 34.9%, compared with state-of-the-art sensing methods in FD systems, suffering from residual SI and CFO.**

***Index Terms*—Full Duplex, cognitive radio network, spectrum sensing, OFDM, self-interference.**

I. Introduction

In recent years, in-band full-duplex (FD) wireless technology has attracted significant interest in its application to cognitive radio networks (CRNs). Unlike the half-duplex (HD) radios that follow the traditional "listen before talk" (LBT) principle, the FD technique enables simultaneous transmission and reception/sensing on the same frequency channel, referred to as the "listen and talk" (LAT) [1], [2]. In other words, under the LAT protocol, unlicensed secondary users (SUs) can sense the presence of incumbent users (IUs) while transmitting its data packets using the same time and frequency resources (when IUs is absent). That thereby significantly enhance the sensing efficiency as well as increase the system throughput [3].

Although the FD technique or LAT is promising for CRNs, it suffers from a crucial, yet inherent problem: the self-interference (SI) [4]. Various self-interference suppression methods, e.g., advanced time-domain interference cancellation [5], signal inversion and adaptive cancellation [6] and antennas cancellation [7], have been investigated. However, none of these works can guarantee perfect SI suppression performance and the residual SI is still inevitable [8].

Sensing the IU activity states (i.e., absence or presence) with the presence of the residual SI in FD systems is challenging. This is because the residual SI can lead to a low signal-to-interference-plus-noise ratio (SINR) and severely affect the test statistics of sensing methods. One of the most basic spectrum sensing methods in FD systems is the energy detection (ED). However, it is very much susceptible to the noise uncertainty [9]. Although some sensing methods that utilize special features of Orthogonal Frequency Division Modulation (OFDM) signals (e.g., Pilot Tone, PT) are able to achieve better sensing performance, they are greatly vulnerable to the carrier frequency offset (CFO) [10], [11]. A small synchronization error in the frequency domain can result in significant performance degradation [12]. To estimate and mitigate the effect of CFO, a number of highly complex resources and processes are required, posing significantly high complexity. Another main barrier for these sensing methods is that it is extremely difficult to achieve good sensing performance under low signal-to-noise ratio (SNR) conditions. Given the above, this work proposes a novel OFDM signal sensing method in the FD system by leveraging the PT feature that is robust to the residual SI and CFO with low computational complexity. Our major contributions are summarized as follows.

- We investigate OFDM sensing methods in FD systems under low SNR conditions, in the presence of residual SI and CFO. We develop a novel OFDM sensing approach drawing support from the PT feature of OFDM signals. In comparison with other conventional spectrum sensing methods, the proposed sensing approach is more robust to the residual SI and CFO. Additionally, our approach is capable of achieving much higher sensing accuracies under the low SNR condition with lower complexity.
- In contrast to conventional PT-based sensing methods which require complex estimation processes to estimate the impact of the CFO, the presented sensing approach is able to completely avoid such a requirement, significantly reducing the computational complexity.
- For analyzing the performance of our proposed approach, we take two types of residual SI: the residual SI that has the PT structure and the residual SI that does not hold a PT feature. For each type of residual SI, we derive the closed-form expressions of the probability of miss

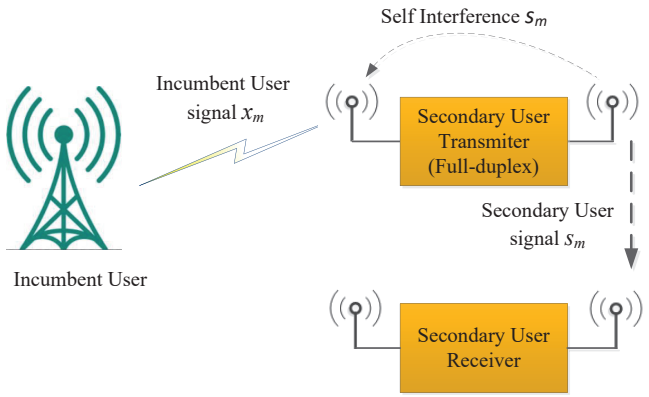

Fig. 1. System model of FD: SU is in "Listen and Talk" mode .

detection and false alarm of the proposed approach.

- Extensive simulations are conducted to validate the effectiveness of our developed method. Simulation results demonstrate that the proposed approach is able to achieve a much higher sensing accuracy with lower complexity under low SNR conditions.

The remainder of this work is organized as follows. Section II describes the system model and problem formulation. The proposed sensing approach is expressed in Section III. The simulation results are shown in Section IV, followed by the conclusions in Section V.

II. System Model

Consider a simplified cognitive FD system, as shown in Fig. 1. The IU has the highest priority to utilize the licensed spectrum and transmits OFDM signals. The SU works in the full-duplex mode, e.g, simultaneously sensing the licensed spectrum and using that licensed channel (when IU is absent) for its data transmission. The SU transmits two types of signals: OFDM signals or other modulation signals, as will be discussed in Section III-A. At the IU transmitter side, the transmitted OFDM signal is given by

$$x_m(n) = \sqrt{\frac{E_s}{N_d}} \sum_{k=0}^{N_d-1} I_m(k) e^{j2\pi nk/N_d}, n \in [-N_c, N_d - 1] \tag{1}$$

where $m = 0, \ldots, M-1$ and M denotes the total number of transmitted OFDM blocks. E_s stands for the transmitted power of each symbol. N_d is the data block size. $I_m(k)$ represents the symbol modulating the kth subcarrier with unit variance. After passing through a multipath fading channel with L uncorrelated taps, the received signal at the SU transmitter, denoted by $y_m(n)$, is expressed as

$$\begin{aligned} H_0 &: y_m(n) = r_m(n) + w_m(n), \\ H_1 &: y_m(n) = e^{\frac{j2\pi f_q n}{N_d}} \sum_{l=0}^{L-1} h_l x_m(n-l) + r_m(n) + w_m(n), \end{aligned} \tag{2}$$

where H_0 refers to the null hypothesis standing for the absence of IU. H_1 is the alternate hypothesis denoting the presence of IU. $r_m(n) \sim CN(0, \sigma_r^2)$ represents the residual SI after self-interference suppression, which can be expressed as $r_m(n) = \delta s_m(n)$, where $s_m(n)$ is the self-interference signal (transmitted signal from SU), and δ refers to the SIS factor [13]. $w_m(n)$ stands for the complex additive white Gaussian noise with zeros mean and σ_w^2 variance. f_q represents the CFO normalized to the subcarrier spacing. $h_l \sim CN(0, 1)$ denotes the channel gain of the lth channel component.

As discussed previously, the received signals are collected for detecting the activity states of IU (i.e., presence or absence). However, from equation (2), it is clear that the residual SI signals are involved in the received signals under both H_0 and H_1, thereby notably degrading the sensing performance in FD systems. Although some feature-based sensing methods (e.g., leveraging PT features [10]) can be applied to achieve better sensing methods with the residual SI, they are sensitive to CFO that causes dramatic performance degradation. To address this problem, in the next section, we develop a novel sensing method to overcome the adverse effect of the residual SI and CFO.

III. The Proposed Pilot-Tone Based Spectrum Sensing Approach

In this section, the details of our proposed spectrum sensing algorithm based on the PT feature of OFDM signals are firstly provided. We then derive theoretical expressions of the probability of miss detection (P_m) and false alarm (P_f) of our developed sensing approach.

Given an OFDM system, PTs are always designed/added to meet the channel estimation requirement. In this work, we adopt a circular configuration type of PT [14], meaning that the pilot symbols are the same every serval blocks but different in one block. Besides, all PTs signals have the same amplitude. As a result, the correlation features between PTs can provide unique features that can be utilized to sense the presence of IU. Furthermore, in order to utilize the PT feature for sensing purpose, the received time domain signal should be converted into frequency domain. Specifically, the discrete Fourier transform of the received signal (the cyclic prefix (CP) structure is already discarded) can be written as

$$\widetilde{Y}_m(k) = U_m(k) + R_m(k) + W_m(k), \tag{3}$$

where

$$\begin{aligned} U_m(k) &= \sum_{n=0}^{N_d-1} \sqrt{E_s} \Delta_{f_q}(n-k) H(n) I_m(n), \\ \Delta_{f_q}(i) &= \frac{sin(\pi f_q)}{sin(\frac{\pi}{N_d}(f_q+i))} \exp(j\frac{\pi}{N_d}((N_d-1)f_q - i)), \end{aligned} \tag{4}$$

here $H(n) = \sum_{l=0}^{L-1} h_l e^{-j2\pi ln/N_d}$ represents the frequency response of the nth subcarrier. $R_m(k) \sim CN(0, \sigma_r^2)$ and $W_m(k) \sim CN(0, \sigma_n^2)$ denotes the residual SI and noise in the frequency domain, respectively. Since the signal of IU has the circular configuration PT structure, $\widetilde{Y}_m$ and $\widetilde{Y}_s$ have the same PT arrangement if $m - s = dv, d = 1, 2, 3 \ldots$, where v is

the circular period. On the basis of this feature, the proposed new cross-correlation matrix is given by

$$\mathbf{C} = \frac{1}{N_v} \sum_{N_v} \widetilde{\mathbf{Y}}_m^{PT} (\widetilde{\mathbf{Y}}_s^{PT})^*, \tag{5}$$

where $\mathbf{C}$ stands for the cross-correlation matrix of size $N_p \times N_p$. N_p is the length of PT. $\widetilde{\mathbf{Y}}_m^{PT}$ denotes the PT vector in the mth OFDM block. N_v is defined as $N_v = \lceil \frac{M-1}{2v} \rceil (2M - v - v\lceil \frac{M-1}{v} \rceil)$ representing the total number of OFDM block pairs (m, s) with the same PT arrangement. $(.)^*$ means the conjugate transpose.

Note that in (5), the proposed cross-correlation matrix only computes the the pilot tones but ignores other transmitted symbols, which is able to remove the correlation noise and reduce the effect of residual SI. Thus the test statistic of proposed method can be written as

$$T = \frac{1}{N_p^2} \sum_{p=0}^{N_p-1} \sum_{q=0}^{N_p-1} |C(p,q)|^2 \tag{6}$$

A. Probability of False Alarm and Detection

In this section, the expressions of the probability of false alarm (P_f) and miss detection (P_m) for the proposed algorithm are derived based on the test statistic provided previously. According to equation (6), T is the the sum of N_p^2 variables ($|C(p,q)|^2$). Thus in order to get the distribution of T, the statistic features of $C(p,q)$ should be discussed first. Since $C(p,q)$ is the value of cross-correlation of PT structures, statistical characteristics of $C(p,q)$ are depend on whether the received signals have PT structures or not. For the noise signal, it does not have a PT structure, so its effect on test statistics is quite small. Regarding the residual SI signal (i.e., SU's transmitted signal), it is possible to have the PT structure, so it is desirable to discuss the structure of residual SI for achieving satisfactory sensing performance. In the following parts, we consider two different cases: residual SI signals have no PT structure and residual SI signals have the PT structure.

1) Case A: Residual SI signals without PT structure

In this scenario, for deriving the probability distribution function (*pdf*) of T, we first calculate the means and variances of $C(p,q)$ in hypotheses H_0 and H_1. Under H_0, since the received signal only contains the residual SI signal and noise, $C(p,q)$ can be expressed as:

$$C(p,q)|H_0 = \frac{1}{N_v} \sum_{N_v} \big(R_m(p) + W_m(p)\big)\big(R_s(q) + W_s(q)\big)^*. \tag{7}$$

As the residual SI signal has no PT structures, $R_m(p)$ is independent of $R_s(q)$. Besides, as mentioned previously, the residual SI signal and noise are independent of each other, hence, the mean and variance of $C(p,q)$ can be obtained by

$$\mu_0(p,q) = \mathrm{E}[\frac{1}{N_v} \sum_{N_v} \big(R_m(p) + W_m(p)\big)\big(R_s(q) + W_s(q)\big)^*] = 0, \tag{8}$$

$$\sigma_0^2(p,q) = \mathrm{E}[|C(p,q)|^2 | H_0] - \mu_0^2(p,q) = \frac{(\sigma_n^2 + \sigma_r^2)^2}{N_v}. \tag{9}$$

Under H_1, according to equation (3), $C(p,q)$ can be written as

$$\begin{aligned} C(p,q)|H_1 &= \frac{1}{N_v} \sum_{N_v} \big(U_m(p) + R_m(p) + W_m(p)\big) \\ &\quad \times \big(U_s(q) + R_s(q) + W_s(q)\big)^*. \end{aligned} \tag{10}$$

As discussed above, for the PT structure of the IU signal, if block index difference $m - s = dv, d = 1, 2, 3 \ldots$, then two OFDM blocks have the same PT arrangement. Thus the mean of $C(p,q)$ is

$$\begin{aligned} \mu_1(p,q) &= \mathrm{E}[C_s(p,q)|H_1] \\ &= E_s \sum_{n=0}^{N_d-1} |H(n)|^2 \Delta_{f_q}(n-p) \Delta_{f_q}(n-q)^*. \end{aligned} \tag{11}$$

The variance of $C(p,q)$ can be given by

$$\sigma_1^2(p,q) = \mathrm{E}[|C(p,q)|^2 | H_1] - \mu_1^2(p,q). \tag{12}$$

Since the SU intends to sense the licensed spectrum under low SNR condition, when M is lager, $\sigma_1^2(p,q)$ can be approximated by

$$\begin{aligned} \sigma_1^2(p,q) &= \frac{3E_s^2}{N_v} \sum_{n=0}^{N_d-1} |H(n)|^4 |\Delta_{f_q}(n-p)|^2 |\Delta_{f_q}(n-q)|^2 \\ &\quad + \frac{E_s(\sigma_n^2 + \sigma_r^2)}{N_v} \Big(\sum_{n=0}^{N_d-1} |H(n)|^2 |\Delta_{f_q}(n-p)|^2 \\ &\quad + |\Delta_{f_q}(n-q)|^2 \Big) + \frac{(\sigma_r^2 + \sigma_n^2)^2}{N_v}. \end{aligned} \tag{13}$$

2) Case B: Residual SI signals hold the same PT structure as IU

In this case, we assume the residual SI signals have the same PT arrangement as the IU signals. Thus when $m - s = dv$ $(d = 1, 2, 3 \ldots)$, $R_m(p)$ is equal to $R_s(p)$, $p = [0, 1, \ldots, N_p - 1]$, implying that the residual SI signal causes a great impact on the value of $C(p,q)$. In such a case, the mean and variance of $C(p,q)$ under H_0 can be obtained according to equation (7):

$$\mu_0(p,q) = \mathrm{E}[C(p,q)|H_0] = \sigma_r^2, \tag{14}$$

$$\begin{aligned} \sigma_0^2(p,q) &= \mathrm{E}[|C(p,q)|^2 | H_0] - \mathrm{E}[C(p,q)|H_0]^2 \\ &= \frac{1}{N_v} (\sigma_n^4 + 2\sigma_n^2 \sigma_r^2). \end{aligned} \tag{15}$$

The mean and variance of $C(p,q)$ under H_1 can be obtained by following similar derivation processes provided in the previous section, which are

$$\mu_1(p,q) = E_s \sum_{n=0}^{N_d-1} |H(n)|^2 \Delta_{f_q}(n-p) \Delta_{f_q}(n-q)^* + \sigma_r^2, \tag{16}$$

$$\sigma_1^2(p,q) = \frac{3E_s^2}{N_v}\sum_{n=0}^{N_d-1}|H(n)|^4|\Delta_{f_q}(n-p)|^2|\Delta_{f_q}(n-q)|^2 + \frac{E_s(\sigma_n^2+3\sigma_r^2)}{N_v}\Big(\sum_{n=0}^{N_d-1}|H(n)|^2|\Delta_{f_q}(n-p)|^2 + |\Delta_{f_q}(n-q)|^2\Big) + \frac{2\sigma_r^2\sigma_n^2+\sigma_n^4}{N_v}. \quad (17)$$

Based on all the derivations above, the means and variances of $C(p,q)$ in two special cases can be calculated. According to the central limit theorem, $C(p,q)$ can be approximated as complex Gaussian variable ($C(p,q) \sim CN(\mu(p,q),\sigma^2(p,q))$) when M is large under both H_0 and H_1. As a result, $2|C(p,q)|^2/\sigma^2(p,q)$ obeys non-central Chi-square distribution with $2|\mu(p,q)|^2/\sigma^2(p,q)$ non-centrality parameter and two degree of freedom [15]. So the test statistic in equation (6) can be rewritten as

$$T' = \frac{1}{N_p^2}\sum_{p=0}^{N_p-1}\sum_{q=0}^{N_p-1}\frac{2|C(p,q)|^2}{\sigma^2(p,q)} \underset{H_1}{\overset{H_0}{\lessgtr}} \gamma, \quad (18)$$

where γ is the threshold. According to equation (18), T' is the sum of N_p^2 independent and identically distributed non-central Chi-square variables. Thus T' obeys noncentral Chi-square distribution with $2N_p^2$ degree of freedom. The non-central parameters and the probability distribution function of T' under H_0 and H_1 are equal to

$$\lambda_{T',0} = \sum_{p=0}^{N_p-1}\sum_{q=0}^{N_p-1}\frac{2|\mu_0(p,q)|^2}{\sigma_0^2(p,q)},$$
$$\lambda_{T',1} = \sum_{p=0}^{N_p-1}\sum_{q=0}^{N_p-1}\frac{2|\mu_1(p,q)|^2}{\sigma_1^2(p,q)}, \quad (19)$$

$$f(T';\eta,\lambda_{T',i}) = \frac{1}{2}e^{\frac{-(T'+\lambda_{T',i})}{2}}\Big(\frac{T'}{\lambda_{T',i}}\Big)^{\frac{\eta-2}{4}}B_{\frac{\eta-2}{2}}\big(\sqrt{\lambda_{T',i}T'}\big), \quad (20)$$

where $i = 0, 1$. η denotes the degree of freedom. $B_\alpha(\theta)$ stands for the modified Bessel function of first kind defined as $B_\alpha(\theta) = (\frac{\theta}{2})^\alpha\sum_{j=0}^{\infty}[(\frac{\theta^2}{4})^j/j!\Gamma(\alpha+j+1)]$ and Γ denotes the Gamma function. The cumulative distribution function of T' can be calculated as

$$F(T';\eta,\lambda_{T',i}) = \sum_{j=0}^{\infty}e^{\frac{-\lambda_{T',i}}{2}}\frac{\Lambda(\eta/2+j,T'/2)}{\Gamma(\eta/2+j)}\frac{(\lambda_{T',i}/2)^2}{j!}, \quad (21)$$

where Λ denotes the lower incomplete Gamma function.

Based on the derivations and definitions above, the expressions of P_f and miss detection P_d can be obtained by

$$P_f = 1 - F(\gamma; 2N_p^2, \lambda_{T',0}),$$
$$P_m = F(\gamma; 2N_p^2, \lambda_{T',1}). \quad (22)$$

According to the Neyman-Pearson criterion [16], the performance of the proposed sensing method can be evaluated by fixing P_f to obtain the threshold γ which is

$$\gamma = F^{-1}(1 - P_f; 2N_p^2, \lambda_{T',0}), \quad (23)$$

TABLE I
COMPUTATIONAL COMPLEXITY OF DIFFERENT SENSING METHODS

Method	Number of complex multiplications
SCM [10]	$MN_d\log(N_d) + MN_d^2$
FD-AC [11]	$MN_{FFT}\log(N_{FFT}) + 2MN_{comp}$
Proposed method	$MN_d\log(N_d) + N_vN_p^2$

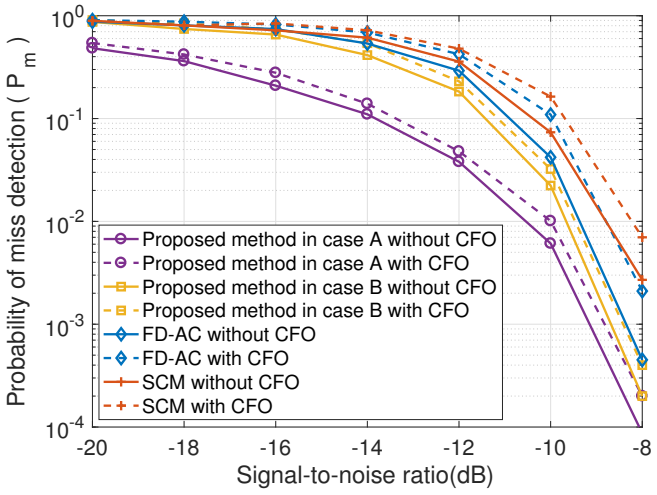

Fig. 2. Impact of CFO on probability of miss detection (P_m) of various sensing methods.

B. Computational Complexity

In this section, we compare the computational complexity of the proposed sensing approach with other relevant sensing methods, e.g., sampled covariance matrix (SCM) [10] and frequency domain autocorrelation (FD-AC) [11], as shown in Table I.

We select the number of complex multiplications as a metric to validate the computational complexity because it is the most computationally expensive. In Table I, N_{FFT} and N_{comp} stand for the FFT size and the number of used subcarriers (denoted as K and K_{comp} in [11]), respectively. As can be seen from this table, our proposed method costs a much less number of complex multiplications, compared to the other two sensing methods. For instance, when $N_d = 64$, $M = 20$, $N_p = 16$, $v = 3$, $N_{FFT} = 1024$ and $N_{comp} = 242$, the total number of complex multiplications of SCM [10] and FD-AC [11] are 87243 and 151640, respectively. By contrast, that number of the proposed sensing method is only 19915, much lower than the other two sensing methods.

IV. Simulation Results

In this section, we validate the performance of the proposed spectrum sensing approach using P_m as a metric. The numerical results are given via Monte Carlo simulations in the FD system. Unless otherwise stated, the simulation configurations are set as follows. The binary phase shift keying (BPSK) modulation is applied to generate an OFDM system. We assume the number of received OFDM blocks is $M = 20$, and the data block size of the received OFDM signals is $N_d = 64$.

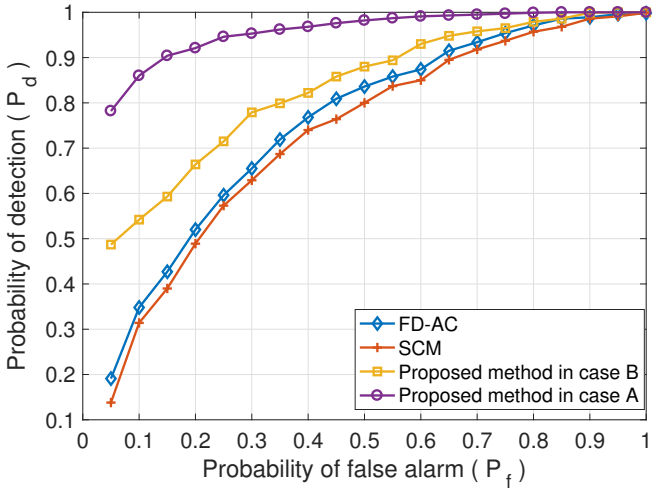

Fig. 3. ROC curves for different detectors at SNR = -15 dB

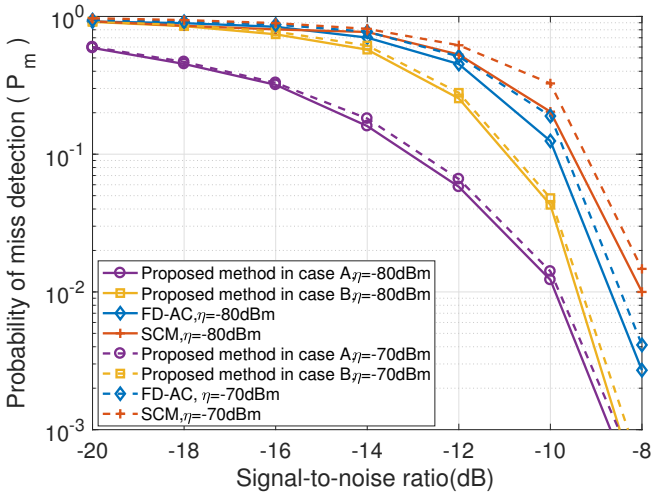

Fig. 4. The impact of residual SI on probability of miss detection (P_m) of different sensing methods

The length of the PT structure is set as $N_p = 16$ with circular period $v = 3$. The operating radio frequency is 2.4 GHz, and the signal bandwidth is set to be 5 MHz. The spacing for each subcarrier is 78.125 kHz. SNR varies in the range of $-20 \backsim -8$dB, and the normalized CFO is evenly distributed in $[-0.5, 0.5)$. The residual SI power at SU's transmitter η is set to be -87dBm adopting the self-interference suppression method proposed in [17]. The value of the probability of false alarm (P_f) is set as 0.05.

In Fig. 2, we compare the probability of miss detection (P_m) of our proposed approach with the other two sensing methods, e.g., SCM [10] and FD-AC [11]. As can be seen, our presented approach for both Cases A and B significantly outperforms the other two methods regardless of whether CFO is present or not. Although all the sensing methods are affected by CFO, the impact on our developed approach is much less compared with the other two methods. The figure also shows that our proposed approach for Case A can achieve better sensing performance, i.e., lower P_m, than Case B. This is because the residual SI signal in the Case A has no PT structure, hence, its impact on $\mathbf{C}$ is less than that in the Case B (refer to equation (5)), leading to higher sensing accuracy.

To further evaluate the sensing performance, we show the operating characteristic (ROC) curves for various algorithms at SNR $= -15$dB in Fig. 3. As can be seen, this figure illustrates the relationship between the probability of detection (P_d, $P_d = 1 - P_m$) and the probability of false alarm (P_f). We can observe that our proposed sensing approach clearly outperforms the other two methods. In particular, with a fix P_f, the two cases of our proposed approach are capable of achieving much better sensing accuracy (i.e., higher P_d) compared with the other two sensing methods. When $P_f = 0.05$, P_d of our proposed algorithm in Case A and Case B are 0.782 and 0.487, respectively. However, P_d of FD-AC [11] and SCM [10] methods are only 0.191 and 0.138, respectively.

From Fig. 2 and Fig. 3, we can obtain an observation that either P_m or ROC is able to show the sensing performance of various sensing methods. Due to the space limitation, in the sequel, we will only discuss P_m.

Fig. 4 demonstrates the P_m performance of various methods in the presence of residual SI. From this figure, it is apparent that our presented algorithm is superior to others regarding the robustness to residual SI. Besides, the sensing performance of our method in Case A is better than in Case B because of different types of residual SI signals. When SNR is -10dB, as the residual SI power η rises from -80dBm to -70dBm, P_m of our designed approach in the Case A and Case B increase from 0.0122 to 0.0141, and from 0.0429 to 0.0480, respectively. However, P_m of SCM [10] and FD-AC [11] increase from 0.2035 to 0.3263, and from 0.1247 to 0.1892, respectively.

Fig. 5 illustrates the impact of the number of received OFDM blocks M on the sensing accuracy of various sensing methods. Obviously, our proposed sensing approach in both two cases can achieve much more significant improvements in sensing accuracy (i.e., smaller P_m) with increasing M, compared with the other methods. Moreover, for each sensing method, increasing M can lead to a better sensing performance, while this comes at the cost of higher computational complexity.

In Fig. 6, we present the impact of different PT lengths (N_p) on sensing accuracy. We see from this figure that the length of PT can greatly affect the sensing performance of our proposed method in both two cases. For instance, as N_p increases, a smaller P_m, i.e., better sensing performance, can be achieved. Take Case A as an instance, P_m decreases from 0.156 to 0.004 with increasing N_p from 8 to 32. However, it is worth noting that a larger N_p leads to higher computational complexity.

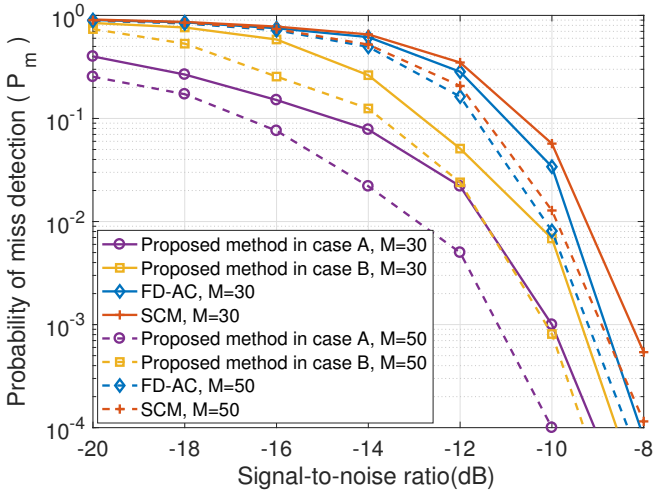

Fig. 5. Probability of miss detection (P_m) of the proposed method with a different number of blocks, M.

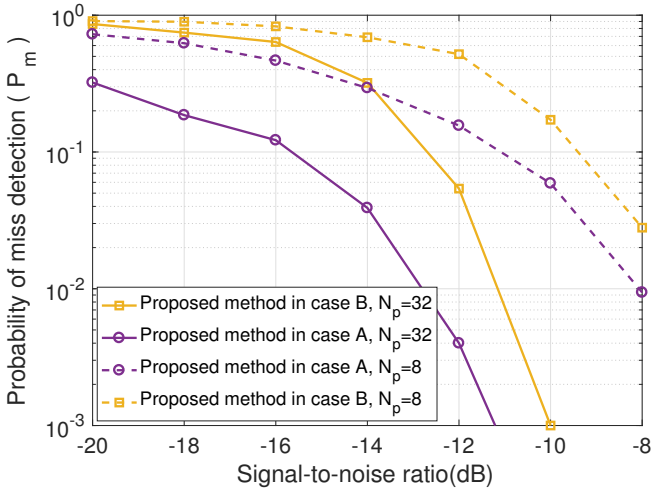

Fig. 6. Probability of miss detection (P_m) of the proposed method with different PT lengths (N_p).

V. Conclusion

We investigated the OFDM spectrum sensing in full-duplex systems in the presence of residual self-interference (SI) and carrier frequency offset (CFO). We proposed a novel OFDM sensing method by leveraging the PT feature of OFDM signals. Besides, two different types of residual SI signals (with or without a PT structure) are taken into account when analyzing the sensing performance of the proposed method. We obtained the closed-form expressions of the probability of miss detection and false alarm of the presented approach. Extensive simulation results demonstrated that our proposed sensing method is more robust to the residual SI and CFO than the conventional ones. Additionally, the proposed method can achieve better sensing performance under the low SNR condition with much lower computational complexity.

References

[1] Y. Liao, T. Wang, L. Song, and Z. Han, "Listen-and-talk: Protocol design and analysis for full-duplex cognitive radio networks," *IEEE Transactions on Vehicular Technology*, vol. 66, no. 1, pp. 656–667, Jan 2017.

[2] S. K. Sharma, T. E. Bogale, L. B. Le, S. Chatzinotas, X. Wang, and B. Ottersten, "Dynamic spectrum sharing in 5g wireless networks with full-duplex technology: Recent advances and research challenges," *IEEE Communications Surveys Tutorials*, vol. 20, no. 1, pp. 674–707, Firstquarter 2018.

[3] Y. Liao, L. Song, Z. Han, and Y. Li, "Full duplex cognitive radio: a new design paradigm for enhancing spectrum usage," *IEEE Communications Magazine*, vol. 53, no. 5, pp. 138–145, May 2015.

[4] Z. Zhang, X. Chai, K. Long, A. V. Vasilakos, and L. Hanzo, "Full duplex techniques for 5g networks: self-interference cancellation, protocol design, and relay selection," *IEEE Communications Magazine*, vol. 53, no. 5, pp. 128–137, May 2015.

[5] S. Hong, J. Brand, J. I. Choi, M. Jain, J. Mehlman, S. Katti, and P. Levis, "Applications of self-interference cancellation in 5g and beyond," *IEEE Communications Magazine*, vol. 52, no. 2, pp. 114–121, February 2014.

[6] M. Jain, J. I. Choi, T. Kim, D. Bharadia, S. Seth, K. Srinivasan, P. Levis, S. Katti, and P. Sinha, "Practical, real-time, full duplex wireless," in *Proceedings of the 17th annual international conference on Mobile computing and networking (MobiCom)*. ACM, 2011, pp. 301–312.

[7] A. Sabharwal, P. Schniter, D. Guo, D. W. Bliss, S. Rangarajan, and R. Wichman, "In-band full-duplex wireless: Challenges and opportunities," *IEEE Journal on Selected Areas in Communications*, vol. 32, no. 9, pp. 1637–1652, Sep. 2014.

[8] C. Politis, S. Maleki, C. G. Tsinos, K. P. Liolis, S. Chatzinotas, and B. Ottersten, "Simultaneous sensing and transmission for cognitive radios with imperfect signal cancellation," *IEEE Transactions on Wireless Communications*, vol. 16, no. 9, pp. 5599–5615, Sep. 2017.

[9] T. Riihonen and R. Wichman, "Energy detection in full-duplex cognitive radios under residual self-interference," in *2014 9th International Conference on Cognitive Radio Oriented Wireless Networks and Communications (CROWNCOM)*, June 2014, pp. 57–60.

[10] W. Xu, W. Xiang, M. Elkashlan, and H. Mehrpouyan, "Spectrum sensing of ofdm signals in the presence of carrier frequency offset," *IEEE Transactions on Vehicular Technology*, vol. 65, no. 8, pp. 6798–6803, Aug 2016.

[11] S. Dikmese, Z. Ilyas, P. C. Sofotasios, M. Renfors, and M. Valkama, "Sparse frequency domain spectrum sensing and sharing based on cyclic prefix autocorrelation," *IEEE Journal on Selected Areas in Communications*, vol. 35, no. 1, pp. 159–172, Jan 2017.

[12] D. Cohen and Y. C. Eldar, "Sub-nyquist cyclostationary detection for cognitive radio," *IEEE Transactions on Signal Processing*, vol. 65, no. 11, pp. 3004–3019, June 2017.

[13] W. Afifi and M. Krunz, "Incorporating self-interference suppression for full-duplex operation in opportunistic spectrum access systems," *IEEE Transactions on Wireless Communications*, vol. 14, no. 4, pp. 2180–2191, April 2015.

[14] H. Chen, W. Gao, and D. G. Daut, "Spectrum sensing for ofdm systems employing pilot tones," *IEEE Transactions on Wireless Communications*, vol. 8, no. 12, pp. 5862–5870, December 2009.

[15] Z. Lei and F. P. S. Chin, "Sensing ofdm systems under frequency-selective fading channels," *IEEE Transactions on Vehicular Technology*, vol. 59, no. 4, pp. 1960–1968, May 2010.

[16] S. Y. Tu, K. C. Chen, and R. Prasad, "Spectrum sensing of ofdma systems for cognitive radio networks," *IEEE Transactions on Vehicular Technology*, vol. 58, no. 7, pp. 3410–3425, Sept 2009.

[17] E. Ahmed and A. M. Eltawil, "All-digital self-interference cancellation technique for full-duplex systems," *IEEE Transactions on Wireless Communications*, vol. 14, no. 7, pp. 3519–3532, July 2015.